

Hot-Spot Particle Emission in Deep-Inelastic $^{16}\text{O} + ^{58}\text{Ni}$ Collisions

P.-A. Gottschalk and M. Weström

Fachbereich Physik, Universität Marburg, D-3550 Marburg/Lahn, Germany

(Received 7 September 1977)

Angular and energy distributions of α particles and neutrons resulting from the decay of a hot spot are calculated using a diffusion model for the internal decay of the hot spot and a final-state interaction of the emitted particles with the residual nuclei. The particle spectra are highly disturbed. Consequences for the interpretation of light-particle emission accompanying deep-inelastic collisions in terms of the hot-spot model are pointed out.

A space-time-correlated excitation in the nucleus, the so-called hot spot, has been proposed¹⁻⁴ to occur in nuclear reactions in particular kinematical situations. In the context of preequilibrium phenomena this type of excitation has been studied^{2,3} in peripheral nucleon-nucleus collisions. Because of a large energy transfer in short interaction times one might expect a hot spot to be created in deep-inelastic heavy-ion collisions. In fact, experimental evidence in favor of this picture has been reported.⁴ In this contribution first results of calculations of light-particle spectra accompanying deep-inelastic collisions in the framework of the hot-spot model are presented.

Deep-inelastic collisions of heavy ions are characterized by a large loss of kinetic energy of the relative motion. Also, an appreciable fraction of the relative orbital angular momentum in the entrance channel is transferred⁵ to intrinsic angular momenta and leads to a polarization of the fragments in the exit channel perpendicular to the scattering plane. A hot spot is likely to be in the overlap region of the nuclear fields of the ions and will internally decay. Therefore, we may distinguish three different time scales which are involved in studying the decay of a hot spot by particle emission: the time scale, τ_{rel} , of the relative motion of the two fragments in the exit channel; the period of their intrinsic rotation, τ_{rot} ; and the characteristic time, τ_{R} , of the internal decay of the hot spot.

Because of the large loss of kinetic energy, τ_{rel} is large compared to τ_{R} , which is of the order of 10^{-22} sec,^{2,3} whence it follows that the particles emitted will strongly interact with the nuclear and Coulomb fields of the heavy fragments. The angular momentum transferred leads to rotation times $\tau_{\text{r}\alpha}$ on the order of τ_{R} , so that the particle spectra will reflect the rotational motion of the emitting fragment. Both effects will modify considerably the energy and angular correla-

tions in the particles emitted. It is clear that quantitative and qualitative informations about the hot spot and aspects of the dynamics of deep-inelastic collisions of heavy ions can be obtained by comparing experimental particle distributions with the results of calculations, based on a given model for the decaying hot spot, where all the three time scales, τ_{rel} , τ_{rot} , and τ_{R} , are consistently taken into account.

The purpose of this Letter is to report on calculated in-plane angular and energy correlations of α particles and neutrons accompanying deep-inelastic collisions of ^{16}O and ^{58}Ni at 96 MeV incident energy. The distributions are obtained from classical three-body trajectory calculations taking into account the internal decay of the hot spot and a final-state interaction of the emitted particles with the residual nuclei. Apart from the set of initial conditions, our calculations resemble the investigations concerning long-range α 's emitted in spontaneous fission.⁶ We confine our discussion to those events in which the light particle is observed in coincidence with oxygen. The model is as follows: We assume a sequential process. A hot spot has been created on the target⁴ in the overlap region of the nuclear fields of the colliding ions and becomes apparent after the breakup of the intermediate complex via particle emission. The time of breakup is set deliberately equal to zero. After the breakup until the time t has elapsed both fragments move on classical Rutherford trajectories. At t a light particle with kinetic energy ϵ is emitted in the direction ϑ by the excited target with the probability $P(\epsilon, \vartheta; t)$ which will be specified later on. After t the three particles are treated as point charges and their trajectories are calculated by a numerical integration of Newton's equations. Whenever a trajectory of the emitted particle crosses the density region of one of the residual nuclei the particle is assumed to be absorbed. In this way we simulate the nuclear interaction. Finally, the ob-

served distributions are obtained by summing over the time t .

The Rutherford trajectories are specified by a complete loss of radial motion of the fragments at $t=0$, by the scission radius R_{sc} of the intermediate complex, and by the orbital angular momentum l_f in the exit channel. The probability $P(\epsilon, \vartheta; t)$ in the rest frame of the emitting nucleus is related to the surface temperature $T(R, \vartheta; t)$ of the excited target^{2,3}:

$$P(\epsilon, \vartheta; t) \propto \exp[-(\epsilon + S)/T(R, \vartheta; t)], \quad (1)$$

where S is the binding energy of the emitted particle. The angle ϑ in Eq. (1) is the polar angle of emission in the intrinsic coordinate system of the emitting nucleus. The z axis points at the (peripheral) hot spot. The time-dependent nuclear temperature field $T(R, \vartheta; t)$ is calculated on the basis of the diffusion model^{2,3} with a δ -like initial temperature distribution. As discussed in Ref. 3, the parameters of $T(R, \vartheta; t)$ are fixed as soon as the equilibrium temperature, T_{eq} , is known. As a result of the angular momentum transferred, the intrinsic coordinate system rotates in space with an angular velocity $\vec{\omega}$. We assume complete polarization of the fragments perpendicular to the reaction plane. Furthermore, we assume at present that $\vec{\omega}$ and l_f resemble the sticking case and that the process proceeds via negative-angle scattering.⁷ By integrating the equations of motion of the three particles in the exit channel up to the time t_∞ where no further significant changes in their motion occurs, we obtain the asymptotic configuration (E, Θ, ∞) , which corresponds to the initial one $(\epsilon, \vartheta; t)$ of a particle emitted at t . The final distribution of all the particles emitted at the time t is given by

$$n(E, \Theta)_t = \iint d\vartheta d\epsilon \left| \frac{\partial(\epsilon, \vartheta; t)}{\partial(E, \Theta; \infty)} \right|^{-1} P(\epsilon, \vartheta; t). \quad (2)$$

From the solution of the diffusion equation^{2,3} we know that the temperature field $T(R, \vartheta; t)$ contains fast modes which dominate at times close to $\tau_R/20$ and a slow mode which survives at large times $t \gtrsim \tau_1$, where $\tau_1 = \tau_R/5$. According to this feature, we distinguish a fast and a slow contribution to the time-integrated spectra which are defined as follows:

$$\begin{aligned} N_{fast}(E, \Theta) &= \int_{\tau_0}^{\tau_1} dt n(E, \Theta)_t, \\ N_{slow}(E, \Theta) &= \int_{\tau_1}^{\tau_R} dt n(E, \Theta)_t. \end{aligned} \quad (3)$$

Here τ_0 is the minimum time which has to elapse so that the diffusion approach is applicable, i.e.,

$\tau_0 = 3 \times 10^{-23}$ sec. It is clear that the fast part of the spectrum depends sensitively on the early stages of the time evolution of the nuclear temperature field. To obtain the complete spectrum, Eq. (2) has to be integrated up to τ_L , where $\tau_L \sim 10^{-20}$ sec is the mean lifetime of the excited target:

$$N(E, \Theta) = N_{fast}(E, \Theta) + N_{slow}(E, \Theta) + N_{eq}(E, \Theta),$$

where

$$N_{eq}(E, \Theta) = \int_{\tau_R}^{\tau_L} dt n(E, \Theta)_t$$

is almost isotropic and contains particles whose energy distribution is purely Maxwellian with the temperature $T = T_{eq}$.

It remains to specify the actual values of the parameters for the present calculation. The excitation energy available in the $^{16}\text{O} + ^{58}\text{Ni}$ reaction is 35 MeV from which $T_{eq} = 1.9$ MeV for Ni is deduced.⁴ Assuming grazing angular momentum in the entrance channel and rigid-body rotation, we obtain in the sticking case $\omega = 1.8 \times 10^{21}$ rad sec⁻¹ and $l_f = 23\hbar$ for the intrinsic rotation and orbital angular momentum, respectively. The nuclear relaxation time τ_R was chosen to be $\tau_R = 20\tau_0$ with $\tau_0 = 3 \times 10^{-23}$ sec.^{2,3} The scission radius was set equal to $R_{sc} = R_{Ni} + R_O = 8$ fm. The three-body calculations were terminated at $t_\infty = 10^{-16}$ sec. Linear and angular momenta of the system as well as the total energy were conserved. In particular, the recoil of the emitted particle has not been neglected. Typically, the relative errors in the computer quantities amount to 10^{-3} at $t_\infty = 10^{-16}$ sec.

The calculated in-plane energy and angular distributions of the emitted α particles are shown in Fig. 1. Contour plots of $N_{fast}(E, \Theta)$ and $N_{slow}(E, \Theta)$ in the center-of-mass system are displayed together with their projections onto the energy and angle axis, respectively. Θ is the angle of the emitted particle relative to the detected O^{16} . Positive angles correspond to particles which are observed to the right of O^{16} as seen from the target.

As is seen from Fig. 1, the Coulomb fields of the residual nuclei focus the particles of the fast mode at angles $\Theta_\alpha \sim +50^\circ$ and $\Theta_\alpha \sim -40^\circ$. This focusing is less pronounced for particles of the slow mode, and the shadow region starts to get populated. Because of the rotation of the emitting Ni target a considerable difference in the spectra for positive- and negative-angle results (right-to-left anisotropy). To a good approximation, the slopes of the angular distribution are purely ex-

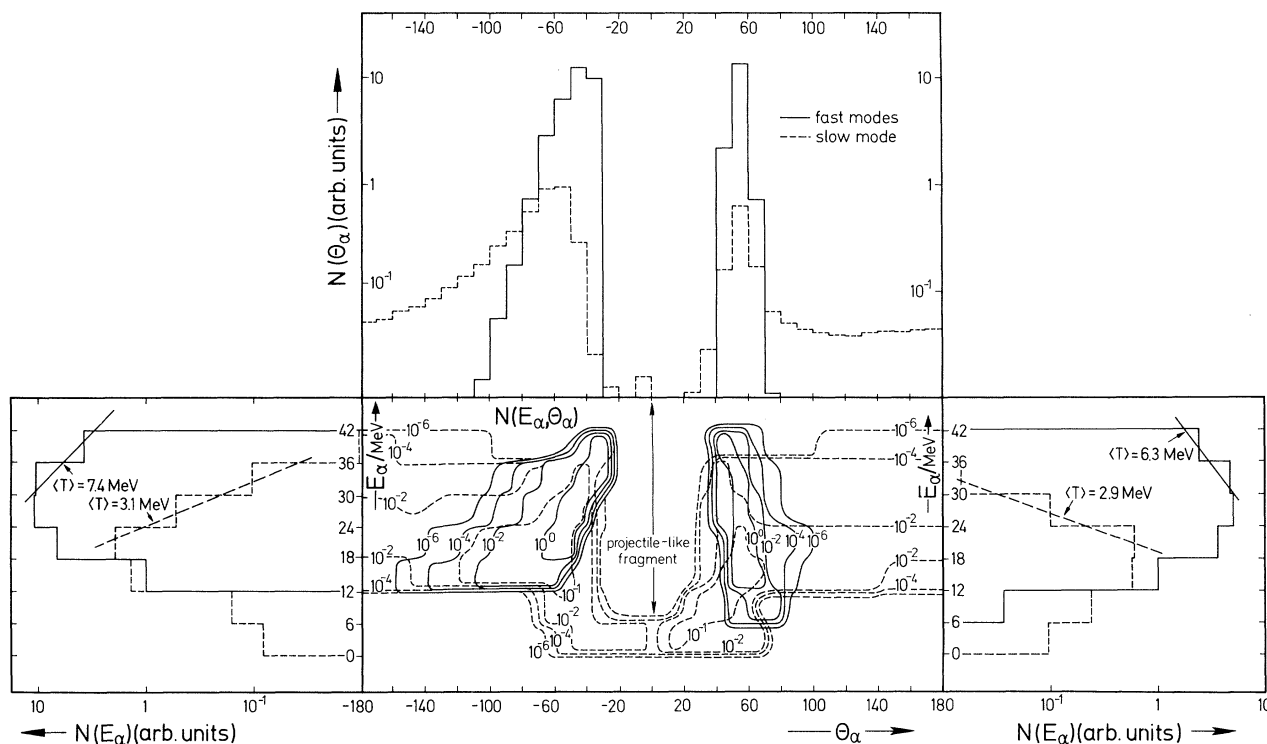


FIG. 1. Calculated center-of-mass angular and energy distributions of α particles accompanying deep-inelastic collisions of ^{16}O with ^{58}Ni at $E_{\text{lab}} = 96$ MeV for the sticking case assuming negative-angle scattering. In the center, contour plots of $N_{\text{fast}}(E_\alpha, \Theta_\alpha)$ and $N_{\text{slow}}(E_\alpha, \Theta_\alpha)$ are displayed, their projections onto the energy axis for angles $\Theta_\alpha \geq 0$ and $\Theta_\alpha \leq 0$ are shown on the right and left, respectively, and the angular distributions are shown at the top; Θ_α is the angle relative to the detected ^{16}O . $\Theta_\alpha > 0$ means angle to the right of ^{16}O as seen from ^{58}Ni .

ponential. It can be shown⁸ that these slopes depend sensitively on the angular gradient of the nuclear temperature field. The nuclear field of the oxygen absorbs a large fraction of fast-mode particles emerging from the hot spot. The resulting angle-averaged energy distribution leads to angle-averaged temperatures of $\langle T_{\text{fast}} \rangle = 6.3$ MeV (7.4 MeV) and $\langle T_{\text{slow}} \rangle = 2.9$ MeV (3.1 MeV) for positive (negative) angles, respectively.

Our calculations are based on a temperature field with a δ -function-like initial temperature distribution. Certainly, the δ -like initial condition simplifies the actual situation and overemphasizes the temperature anisotropies in the early stages of the hot spot. However, effects of this condition on the slow component should be negligible. Calculations based on the rolling-type angular-momentum distribution and positive-angle scattering yield spectra which are approximately obtained from those given in Fig. 1 by replacing $\Theta - \Theta_s$ by $-\Theta + \Theta_s$, where Θ_s denotes the angle of the center of the shadow region.

To study the influence of the Coulomb fields of

the residual nuclei on the distribution of the emitted particles, similar calculations were performed for the reaction $\text{O}^{16} + \text{Ni}^{58} \rightarrow \text{O}^{16} + \text{Ni}^{57} + n$. The anisotropies in $N_{\text{fast}}(E, \Theta)$ remain essentially unaltered. The shadow region is narrower and shifted to more negative angles. The neutrons of the slow mode, however, are distributed almost isotropically. Whereas also early α particles of higher energies are reflected by the Coulomb field of the outgoing oxygen, a comparatively larger fraction of the fast neutrons is absorbed. The average temperatures are lower, namely $\langle T_{\text{fast}} \rangle = 4.9$ MeV (5.9 MeV) and $\langle T_{\text{slow}} \rangle = 2.3$ MeV (3.0 MeV) for positive (negative) angles, respectively.

In conclusion, the Coulomb interaction in the exit channel preserves the specific features of the hot spot. The emitted particles are correlated with the direction of the *outgoing* projectile-like fragment. Although the energy and angular distributions are strongly disturbed, they are still of statistical type. These facts enable one to distinguish experimentally between light parti-

cles produced in a direct reaction and those which result from a hot spot produced in a sequential process. The out-of-plane spectra as well as a generalization of our model with respect to the initial conditions will be presented in a forthcoming paper.⁸

We acknowledge discussions with R. Albrecht, H. Ho, and J. P. Wurm, and the help of T. Ledergerber in the early stages of programming.

¹H. A. Bethe, Phys. Rev. **53**, 675 (1938).

²R. Weiner and M. Weström, Phys. Rev. Lett. **34**, 1523 (1975).

³R. Weiner and M. Weström, Nucl. Phys. **A286**, 282 (1977).

⁴H. Ho, R. Albrecht, W. Dünneberger, G. Graw, S. D. Steadmann, Z. P. Wurm, D. Disdier, V. Rauch, and F. Scheibling, to be published.

⁵P. Glässel, R. S. Simon, R. M. Diamond, R. C. Jared, I. Y. Lee, L. G. Moretto, J. O. Newton, R. Schmitt, and F. S. Stephens, Phys. Rev. Lett. **38**, 331 (1977); R. Albrecht, W. Dünneberger, G. Graw, H. Ho, S. G. Steadmann, and J. P. Wurm, Phys. Rev. Lett. **34**, 1400 (1975).

⁶Y. Boneh, Z. Fraenkel, and I. Nebenzahl, Phys. Rev. **156**, 1305 (1976).

⁷J. Wilczynski, Phys. Lett. **47B**, 484 (1973).

⁸P.-A. Gottschalk and M. Weström, to be published.

nd Scattering at 180° for Neutron Energies from 200 to 800 MeV

B. E. Bonner

Los Alamos Scientific Laboratory, University of California, Los Alamos, New Mexico 87545

and

C. L. Hollas, C. R. Newsom, and P. J. Riley

University of Texas, Austin, Texas 78712

and

G. Glass

Texas A&M University, College Station, Texas 77843

(Received 19 September 1977)

We have measured the cross section for neutron-deuteron elastic scattering over the incident energy range 200–800 MeV. Preliminary results for the extreme back angles ($\theta_n^* \geq 175^\circ$) show a striking shoulder in the excitation function for neutron energies 300–600 MeV. Comparison is made with calculations using the Craigie-Wilkin triangle-diagram technique.

Near the end of the last decade, *pd* elastic scattering experiments demonstrated that the angular distributions were characterized by a strong backward peak in the neighborhood of 1 GeV.¹ Kerman and Kisslinger,² in an attempt to understand this behavior, found that simple one-nucleon exchange failed to fit the backward peak, the calculation being low by a factor of 2. They postulated the existence of isobars in the deuteron, finding that a 1% admixture of the $N^*(1688)$ sufficiently augmented the calculated cross section to bring it into agreement with the 1-GeV data of Bennett *et al.*¹ Since then, several experiments and calculations have been performed relating to backward *pd* elastic scattering at medium energy and isobars in nuclei.³ Alternative explanations of the observed peaking were proposed. One was the calculation of Craigie and

Wilkin⁴ in which triangle diagrams were used to relate the cross sections for *pd* elastic and *pp* $\rightarrow d\pi^+$. Many authors have pursued this technique with success in fitting backward *pd* scattering. Another recent calculation⁵ takes account of the fact that *np* angular distributions also are backward peaked and incorporates this into an extended Glauber multiple-scattering calculation plus one-nucleon exchange. With this approach, backward *pd* scattering is fitted over a wide range of energies above 660 MeV when a radically different form factor for the deuteron is postulated for the large momentum transfers encountered. Recent measurements⁶ at the Stanford Linear Accelerator Center tend to verify the postulated shape of the deuteron form factor.

There are several plots in the literature of the extrapolated 180° cross section as a function of